Technical Note

Heating of Metallic Implants and Instruments Induced by Gradient Switching in a 1.5-Tesla Whole-Body Unit

Hansjörg Graf, PhD, Günter Steidle, MS, and Fritz Schick, PhD, MD*

Purpose: To examine gradient switching–induced heating of metallic parts.

Materials and Methods: Copper and titanium frames and sheets ($\approx 50 \times 50$ mm^2, 1.5 mm thick, frame width = 3 mm) surrounded by air were positioned in the scanner perpendicular to the static field horizontally 20 cm off-center. During the execution of a sequence (three-dimensional [3D] true fast imaging with steady precession [True-FISP], TR = 6.4 msec) exploiting the gradient capabilities (maximum gradient = 40 mT/m, maximum slew rate = 200 T/m/second), heating was measured with an infrared camera. Radio frequency (RF) amplitude was set to zero volts. Heating of a copper frame with a narrowing to 1 mm over 20 mm at one side was examined in air and in addition surrounded by several liters of gelled saline using fiber-optic thermography. Further heating studies were performed using an artificial hip made of titanium, and an aluminum replica of the hip prosthesis with the same geometry.

Results: For the copper specimens, considerable heating (>10°C) in air and in gelled saline (>1.2°C) could be observed. Heating of the titanium specimens was markedly less (≈1°C in air). For the titanium artificial hip no heating could be detected, while the rise in temperature for the aluminum replica was approximately 2.2°C.

Conclusion: Heating of more than 10°C solely due to gradient switching without any RF irradiation was demonstrated in isolated copper wire frames. Under specific conditions (high gradient duty cycle, metallic loop of sufficient inductance and low resistance, power matching) gradient switching–induced heating of conductive specimens must be considered.

Key Words: MR safety; heating; gradient switching; implant; instrument
J. Magn. Reson. Imaging 2007;26:1328–1333.

ONE IMPORTANT ASPECT in MR safety testing of medical implants and instruments is the inspection of whether hazardous heating can occur in the electromagnetic environment of an MR scanner. In the standard ASTM F 2182-02a (1), heating resulting from the interaction with the radio frequency (RF) magnetic field is considered. Numerous examinations have been reported concerning this subject (e.g., Ref. 2–10). Regarding gradient switching, there are a few works that address the alteration of induced nerve stimulation near metallic implants (11,12). Two publications (13,14) ascribe heat sensations of patients with larger metallic implants to vibrations of these implants caused by gradient switching.

In contrast to ASTM F 2182-02a and to those works, the present study is concerned with direct gradient switching–induced heating of medical implants or instruments made of electrically conducting material. Following Faraday's law, the change of the magnetic flux through such a device induces eddy currents in the device and the metal subsequently converts electric energy into thermal energy. This effect increases with distance from isocenter. To obtain insight into the order of magnitude of possible effects, quadratic wire frames and sheets made of copper and titanium were examined. Most experiments were performed in air, since the underlying cause for the heating is pure magnetic induction during gradient switching without any resonance effects. Energy deposition in the metallic parts must be expected to be very similar in air and in aqueous media, since Faraday's magnetic induction depends on the temporal change of magnetic flux only, not on the dielectric properties of the medium. This is clearly different from the well-known RF coupling of metallic structures, where dielectric properties and resulting wave lengths in the medium can play an important role.

The temperature of the parts was monitored with an infrared camera during the execution of a sequence with high gradient duty cycle and with RF pulses switched off.

On the other hand, water as surrounding medium is expected to lead to a clearly better cooling of the metal parts due to its higher heat conductivity and capacity. For this reason we conducted an additional measure-

Section on Experimental Radiology, Department of Diagnostic Radiology, University Hospital Tübingen, Tübingen, Germany.

Contract grant sponsor: German Ministry for Education and Research (BMBF); Contract grant number: 16SV1351.

*Address reprint requests to: F.S., University Hospital Tübingen, Section on Experimental Radiology, Hoppe-Seyler-Str. 3, D-72076 Tübingen, Germany. E-mail: fritz.schick@med.uni-tuebingen.de

Received October 24, 2006; Accepted July 31, 2007.
DOI 10.1002/jmri.21157
Published online in Wiley InterScience (www.interscience.wiley.com).

Table 1
Specific Ohmic Resistance ρ, Specific Heat Capacities *c* and c_V, and Specific Weight *w* of Different Metals and Alloys Used for Medical Equipment and Implants*

Material	ρ (Ω-mm²/m)	*c* [J/(kg/K)]	*w* (g/cm³)	c_V [J/cm³/K]
Cu	0.017	385	8.920	3.43
Ti	0.554	520	4.507	2.34
Ti-6Al-4V	1.7	526	4.420	2.32
NiTi (Nitinol)	0.82	320	6.450	2.43
Al	0.0265	900	2.700	2.06
CoCrNi (Eligiloy/Phynox)	0.996	430	8.300	3.57
316 stainless steel	0.74	500	7.990	4.00

*Sources: Handbook of Chemistry and Physics; for alloys: http://www.matweb.com.
Cu = copper, Ti = titanium, Al = aluminum, V = vanadium, Ni = nickel, Co = cobalt, Cr = chromium.

ment with a copper frame using agar gelled saline as surrounding medium. In this case heating had to be measured using fiber-optic thermography.

MATERIALS AND METHODS

Theory

To investigate eddy-current–induced heating, the specimens were modeled as quadratic frames made of conducting material with l = side length of the frame, A = area of the frame, and q = cross-section of the conductor. Materials with different specific ohmic resistance ρ were taken into account (Cu = 0.017 Ω-mm²/m, Ti = 0.554 Ω-mm²/m, for further relevant material parameters see Table 1).

The voltage U_{ind} induced by changing magnetic flux ϕ through the frame without rotation of the frame (constant effective area A), obeys Faraday's Law:

$$U_{ind} = -\frac{d\Phi}{dt} = -\frac{d}{dt}\int \vec{B}\cdot d\vec{A} = -\int \frac{d\vec{B}}{dt}\cdot d\vec{A}, \quad (1)$$

with B the magnetic field at a certain location and dB/dt its time derivative. The electric DC resistance R of the frame can be calculated from:

$$R = \rho\cdot\frac{C_{frame}}{q} = \rho\cdot\frac{4l}{q} \quad (2)$$

In general, the change of magnetic flux through the frame resulting from the real gradient coil field has to be regarded (not only the z-component, which influences the Larmor frequency of transverse magnetization). If the conductive part is located at a certain distance d from isocenter and a gradient $G = dB/dr$ is switched, the magnetic field at this location changes for a linear gradient ramp of time τ with the rate

$$dB/dt = \Delta B/\tau = G\cdot d/\tau. \quad (3)$$

Since the magnetic field changes relatively fast, maximum eddy current $I_{max} = U_{ind}/R$ can usually not be achieved during the short ramp time due to the inductance L of the metal part. The current at the end of the ramp must be calculated for $t = \tau$ from

$$I_{eddy}(t) = I_{max}(1 - e^{-\kappa\cdot t}), \quad (4)$$

with $\kappa = R/L$ the built-up rate for the eddy current. The inductance L of a frame was estimated according to the formula for a single loop (14):

$$L \approx \mu_0\pi\cdot r_{loop} \approx \mu_0 C_{frame}/2 = \mu_0\cdot 2l. \quad (5)$$

The electric power at a certain time t is given by

$$P(t) = RI^2_{\max}(1 - e^{-\kappa\cdot t})^2. \quad (6)$$

The energy deposited during ramp-up (or ramp-down) in dependence on R at a given inductance L and a fixed U_{ind} can be calculated from

$$\begin{aligned} E(R) &= \int_0^\tau P(t)dt = \frac{U^2_{ind}}{R}\int_0^\tau (1 - e^{-\frac{R}{L}t})^2 dt \\ &= \frac{U^2_{ind}}{R}\left[t + \frac{2L}{R}e^{-\frac{R}{L}t} - \frac{L}{2R}e^{-\frac{2R}{L}t}\right]_0^\tau \\ &= \frac{U^2_{ind}}{R}\left(\tau + \frac{2L}{R}e^{-\frac{R}{L}\tau} - \frac{L}{2R}e^{-\frac{2R}{L}\tau} - \frac{3L}{2R}\right). \end{aligned} \quad (7)$$

At the specific resistance $R = R_{match}$, which depends on the parameters L and τ, power-matching occurs, i.e., $E(R)$ becomes maximal. Analyzing Eq. [7] with respect to the dependence of R_{match} and $E(R_{match})$ on L and τ leads to the following rules: R_{match} and $E(R_{match})$ increase linearly with increasing L. R_{match} increases with $1/\tau$ for shorter τ, whereas $E(R_{match})$ is independent of τ.

The plot of Eq. [7] for L = 0.1 μH, τ = 250 μsec, and U_{ind} = 70 mV is shown in Fig. 1. These values for L, τ, and U_{ind} (resulting in $R_{match} \approx 0.75$ mΩ) correspond with the experimental conditions for the metallic frames reported below.

Experiments

Induced heating by gradient switching was examined for quadratic wire frames as well as for sheets of copper and titanium, respectively.

The frames had an effective edge length of 47 mm and a conducting cross-section of 1.5 × 3 mm² (R_{Cu} = 0.71

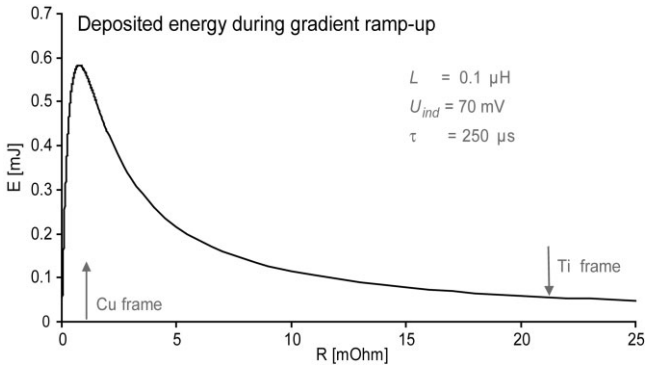

Figure 1. Deposited energy E during gradient ramp-up as a function of the electric resistance R at fixed parameters $L = 0.1$ µH, $\tau = 250$ µsec, $U_{ind} = 70$ mV, corresponding to the metal frames. Power-matching occurs for the copper frame ($R \approx 0.7$ mΩ). The titanium frame shows 32 times higher resistance, clearly resulting in less energy deposition.

mΩ, $R_{Ti} = 23.1$ mΩ), the metal sheets had an edge length of 50 mm and a thickness of 1.5 mm. Additionally, a copper frame with 4-mm frame width and a narrowing to 1 mm over 20 mm at one side was examined. The electric resistances of this frame and of the copper frame with 3-mm frame width were nearly the same. All specimens were covered with a thin layer of mat black spray paint to avoid corrections to the temperature measurement, which would have been necessary for metallic surfaces.

Further heating studies were performed using an artificial hip made of titanium, and an aluminum replica of the hip prosthesis with the same geometry.

All specimens were mounted on blocks of Styrofoam for thermal isolation and were examined inside the scanner in air at approximately 20 cm off-center in the horizontal (x-) direction and perpendicular to the static field. A 2-liter bottle of water placed at isocenter was used as load for the 1.5-T MR scanner (Magnetom Sonata; Siemens, Erlangen, Germany). Heating of the copper frame with the narrowing was also monitored when it was surrounded by 3 liters of gelled saline (1% agar in aqueous solution with 0.9 % NaCl) instead of air.

For temperature monitoring in air an infrared camera (Varioscan high resolution; Jenoptik, Jena, Germany) with a sensitivity of 0.1°C was used. Previous test measurements in comparison with results from a fiber-optic system (LXT Luxtron One; Luxtron, Santa Clara, CA, USA) confirmed the accuracy of the infrared thermometry. The additional heating experiment with the copper frame surrounded by gelled saline was monitored using the above-mentioned fiber-optic probes. In the latter case the infrared camera was not applicable, since infrared light cannot penetrate water, and only the temperature of the water surface can be visualized. The temperatures of the metallic objects and of the gelled saline were carefully adapted to the air temperature in the MR unit before the experiments were started.

Heating of each specimen was monitored for two minutes 10 seconds in copper and titanium frames and plates during the execution of a 3D true fast imaging with steady precession (True-FISP) (fully-balanced steady-state free-precession [SSFP]) sequence, which exploited the gradient capabilities of the scanner (maximum gradient = 40 mT/m, ramp time = 250 µsec, dB/dt = 32 T/second at x = 0.2 m) and which had a high gradient duty cycle (TR = 6.4 msec). Gradient switching in the sequence is indicated in Fig. 2. RF transmitter amplitude was set to zero volts. Transverse slices with frequency encoding in the x-direction were recorded, causing the readout gradient to be mainly responsible for heating in the geometry described above. The same sequence was applied for examinations of the hip prosthesis and its aluminum replica, but the sequence duration was prolonged to three minutes 30 seconds.

The sequence type and positioning of the objects in the scanner were chosen to provide relatively strong but realistic magnetic induction in the objects. The chosen sequence type (3D True-FISP [fully-balanced SSFP]) is often used in clinical routine and works with fast gradient switching along all three main directions (slice, phase, and read direction). The chosen measurement

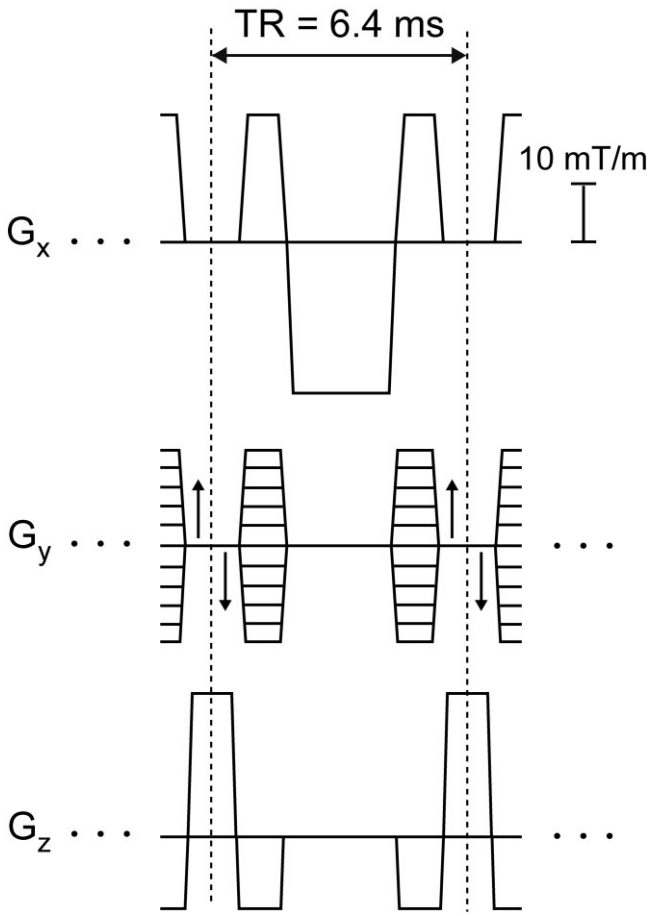

Figure 2. Gradient switching in the 3D-True-FISP (fully-balanced SSFP) sequence. TR was set to 6.4 msec while RF amplitude was zero volts. Since the specimens were mounted at approximately 20 cm off-center in the horizontal (x-) direction, the readout gradients with amplitudes of 28 mT/m and ramp times of 250 µsec were mainly responsible for the gradient-induced heating.

parameters and the positioning of the metallic objects were not especially optimized to get maximum heating effects.

RESULTS

For the copper specimens in air, a considerable warming could be measured (>10°C), whereas for the titanium specimens the rise in temperature was markedly less pronounced (maximally 1°C). Figure 3 shows the infrared images obtained from the Cu sheet and the Cu frames with the True-FISP sequence after a scan time of two minutes 10 seconds (maximum temperature almost reached). For the sheet, a nearly homogenous warming of the complete area was detected (Fig. 3a). Standard deviation (SD) of measured temperature of the copper sheet in a large region of interest (indicated as ROI in Fig. 3a) was only 0.03°C. The frame with the continuous thickness showed heating at the middle of the bars and still more pronounced at the corners (Fig. 3b).

For the frame with a 4-mm frame width and a bar narrowing to 1 mm over 20 mm at one side, the narrowed zone was responsible for enlarged voltage drop and clear heat-up could be observed for the regions adjacent to the narrowing (Fig. 3c). The measurement of the copper frame in gelled saline using fiber-optic thermometry showed clear warming of the copper as indicated in Fig. 4. A series of temperature data recorded prior to the execution of the sequence indicates a slight variation of temperatures due to measuring errors. The precision of the fiber-optic measurements (regarding relative changes in temperature) is approximately 0.1°C. However, the maximum temperature rise in gelled saline was only approximately 1.3°C, compared to more than 10°C in air. Since equal energy disposition is expected for both experiments, the less pronounced temperature rise in gelled saline is probably due to the better cooling capabilities of this surrounding medium.

Examination of the artificial hip replica made of aluminum revealed heating of this massive implant by approximately 2.2°C after three minutes 30 seconds as shown in Fig. 5, whereas the original implant made of titanium did not warm up considerably.

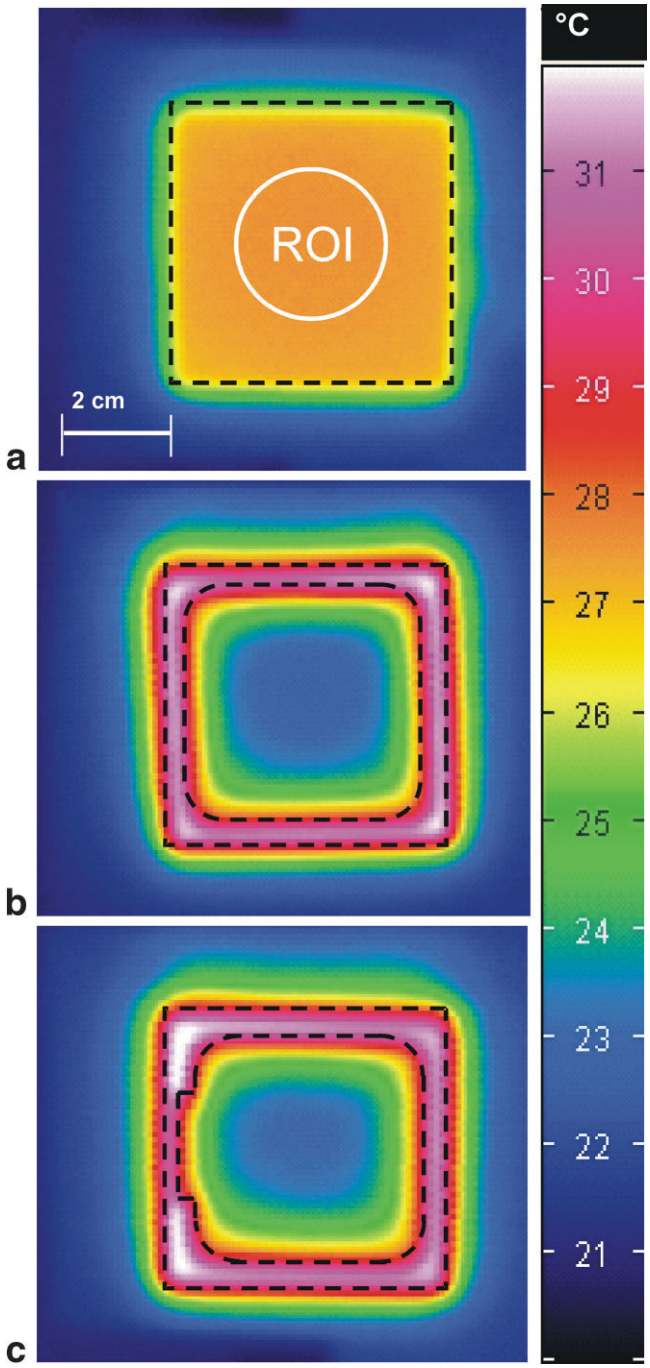

Figure 3. Color-coded infrared images of the Cu specimens obtained after two minutes 10 seconds scanning with the True-FISP sequence with high gradient duty cycle (RF pulses switched off). Copper sheet (**a**), copper frame with constant bar thickness (**b**), and copper frame with bar narrowing at one vertical side (**c**). The shapes of the copper sheet and the frames are indicated by black dotted lines. SD of measured temperature in the ROI in (a) is 0.03°C.

DISCUSSION

RF field–induced heating of tissue near metallic implants or instruments has been examined in several earlier studies and is well understood (2–10). The work presented here shows that for sequences with high gradient duty cycle considerable heating of highly conductive metallic objects as wire frames made of copper can also be generated solely by gradient switching. Furthermore, under specific conditions (high gradient duty cycle, long measuring time, metallic loop of sufficient inductance and low resistance, power matching) gradient switching induced heating of other conductive material such as titanium, nitinol, or 316 stainless steel must be expected.

There are several differences between heating effects caused by gradient switching and those caused by the RF field. Which of the heating effects is dominant depends on the circumstances: RF-related heating is due to E- and B-field coupling with relatively high frequency (63 MHz at 1.5 Tesla). Since resonance effects play an important role it is often very difficult to anticipate RF-related heating in patient examinations. Often a very small change of experimental conditions (e.g., po-

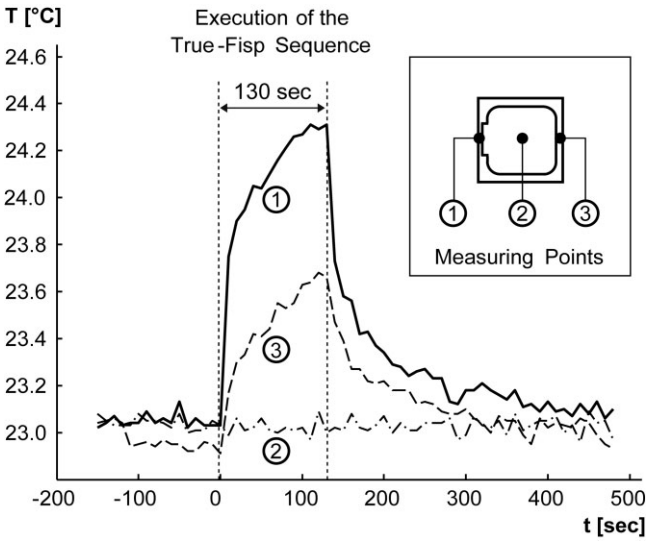

Figure 4. Temperature changes of the Cu frame with bar narrowing at one vertical side positioned in a box filled with gelled saline (1% agar in aqueous solution with 0.9% NaCl). Temperature was measured at three different positions with fiber-optic probes. During the execution of the True-FISP sequence with high gradient duty cycle and a scan time of two minutes 10 seconds, temperature increases up to 1.3°C could be observed using fiber-optic thermography.

sition of the patient in the magnet) might lead to completely changed heating effects. Heating by gradient switching can be more easily calculated applying Faraday's law. Only magnetic flux changes are responsible for induced currents. The relevant frequencies are clearly lower (usually approximately 1 kHz) and resonance effects are not expected. However, in the presence of metallic material both effects might lead to local heating above legal specific absorption rate (SAR) limits under unfavorable circumstances. The dominating heating effect is also dependent on the geometry of the specimen. For example, a straight wire can show heating due to resonant coupling with the E-field components of the RF field, but no heating is expected due to gradient switching. Metallic ring structures allowing eddy currents are usually sensitive to both RF and gradient fields.

The metal object has to allow for eddy currents and must be located at a sufficiently large distance from the isocenter. The electric power from the gradient fields can be converted best to thermal power in the object, if power matching occurs, i.e., if the electric resistance R in the circuit is according to R_{match} in Eq. [7] (dependent on the inductance L of the object and the ramp time τ of the gradient field). For inductances corresponding to typical sizes of metallic implants, R_{match} has to be rather low in the region of several mΩ. This can be achieved by a good conductivity of the material (Cu, Al) or by a large cross-section of the conductor of the loop, if made of worse conducting material (Ti, Nitinol, stainless steel). For example, frame-like metallic vertebral column stabilization (comparable in size to the examined titanium frame) could offer a sufficiently high conductive cross-section (≈1 cm^2). From Eq. [7] it follows that for larger implants power-matching results at higher resistance, and the deposited energy also increases. A shortening of the gradient ramp time τ at constant amplitude leads to higher values R_{match} as well (proportional to $1/\tau$) at constant $E(R_{match})$, i.e., power-matching for an implant or instrument is shifted toward a worse conducting material.

Not only the z-component of magnetic fields generated by the gradient system but also the x- and y-components can be responsible for the induction of heating, and the localization and the orientation of a metallic structure inside or outside the body has to be considered. Voltage and induced currents depend on temporal changes of the total magnetic flux through the wire loop. Unfortunately, only the z-component (along the static field) is well defined, since only the z-component determines the Larmor frequency of the magnetization.

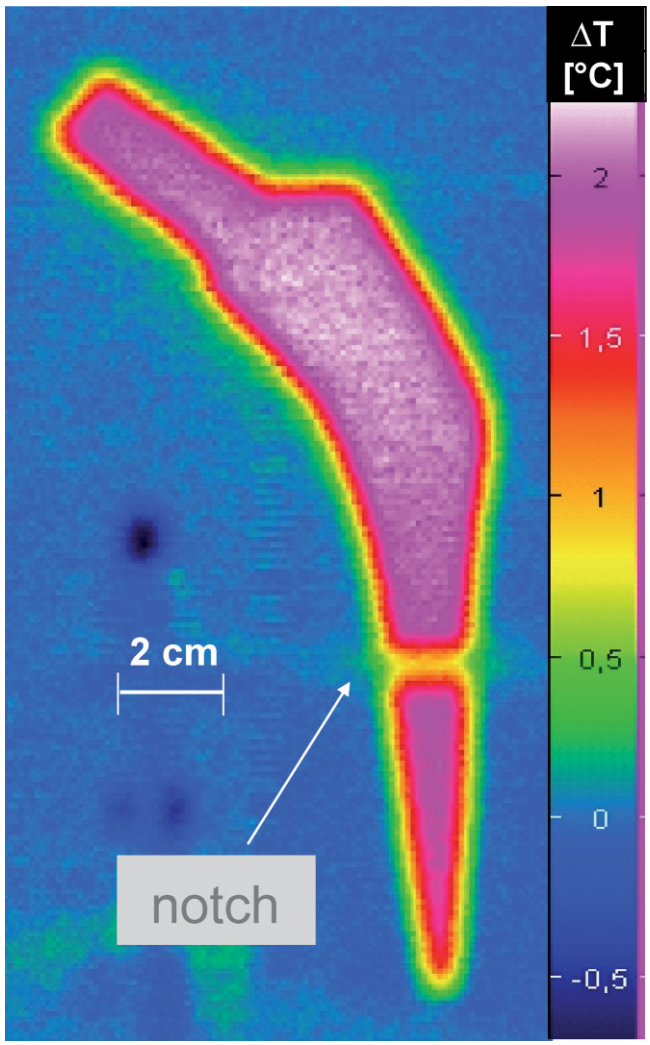

Figure 5. Color-coded ΔT image of the artificial hip replica made of aluminum obtained after three minutes 30 seconds of scanning with the True-FISP sequence with high gradient duty cycle. The entire part warmed up by approximately 2.2°C. An original prosthesis made of titanium did not show measurable warming. [Color figure can be viewed in the online issue, which is available at www.interscience.wiley.com.]

Not only the heating itself, but undesired implant expansion could also cause problematic biological effects due to pressure to the surrounding bony tissue.

To conclude, it was theoretically-derived and experimentally-confirmed that under specific conditions, gradient switching induces heating of metallic implants or instruments. Safety testing of extended implants or instruments should consider potential heating effects with respect to the described mechanisms, especially if they are made of well-conducting materials. For constructing MR-safe medical implants or instruments, beyond low susceptibility of an applied material, low conductivity and/or small cross-sectional areas of ring-shaped devices have to be claimed. Special geometrical constructions of the devices to prevent strong eddy currents could also contribute to solving related problems.

REFERENCES

1. American Society for Testing and Materials (ASTM) Designation: F 2182-02A. Test method for measurement of radio frequency induced heating near passive implants during magnetic resonance imaging. In: Annual Book of ASTM Standards, Section 13, Medical devices and services, vol. 13.01. Medical and surgical materials and devices; anesthetic and respiratory equipment; pharmaceutical application of process analytical technology. West Conshohocken, PA: ASTM; 2002.
2. Nitz WR, Oppelt A, Renz W, Manke C, Lenhart M, Link J. On the heating of linear conductive structures as guide wires and catheters in interventional MRI. J Magn Reson Imag 2001;13:105–114.
3. Smith CD, Kildishev AV, Nyenhuis JA, Foster KS, Bourland JD. Interactions of magnetic resonance imaging radio frequency magnetic fields with elongated medical implants. J Appl Phys 2000;87: 6188–6190.
4. Konings MK, Bartels LW, Smits HFM, Bakker CJG. Heating around intravascular guidewires by resonating RF waves. Magn Reson Imaging 2000;12:79–85.
5. Shellock FG. Metallic neurosurgical implants: evaluation of magnetic field interactions, heating, and artifacts at 1.5-Tesla. J Magn Reson Imaging 2001;14:295–299.
6. Shellock FG. Metallic surgical instruments for interventional MRI procedures: evaluation of MR safety. J Magn Reson Imaging 2001; 13:152–157.
7. Baker KB, Tkach JA, Nyenhuis JA, et al. Evaluation of specific absorption rate as a dosimeter of MRI-related implant heating. J Magn Reson Imaging 2004;20:315–320.
8. Schueler BA, Parrish TB, Lin JC, et al. MRI compatibility and visibility assessment of implantable medical devices. J Magn Reson Imaging 1999;9:596–603.
9. Dempsey MF, Condon B, Hadley DM. Investigation of the factors responsible for burns during MRI. J Magn Reson Imaging 2001;13: 627–31.
10. Shellock FG, Hatfield M, Simon BJ, et al. Implantable spinal fusion stimulator: assessment of MR safety and artifacts. J Magn Reson Imaging 2000;12:214–223.
11. Buechler DN, Durney CH, Christensen DA. Calculation of electric fields induced near metal implants by magnetic resonance imaging switched-gradient magnetic fields. Magn Reson Imaging 1997;15: 1157–66.
12. Reilly JP, Diamant AM. Theoretical evaluation of peripheral nerve stimulation during MRI with an implanted spinal fusion stimulator. Magn Reson Imaging 1997;15:1145–56.
13. Hartwell RC, Shellock FG. MRI of cervical fixation devices: sensation of heating caused by vibration of metallic components. J Magn Reson Imaging 1997;7:771–772.
14. Graf H, Lauer UA, Schick F. Eddy-current induction in extended metallic parts as a source of considerable torsional moment. J Magn Reson Imaging 2006;23:585–590.